Carbohydrate Polymers 95 (2013) 501–507

Contents lists available at SciVerse ScienceDirect

Carbohydrate Polymers

journal homepage: www.elsevier.com/locate/carbpol

Methylene blue adsorption on graphene oxide/calcium alginate composites

Yanhui Li*, Qiuju Du, Tonghao Liu, Jiankun Sun, Yonghao Wang, Shaoling Wu, Zonghua Wang, Yanzhi Xia, Linhua Xia

Laboratory of Fiber Materials and Modern Textile, the Growing Base for State Key Laboratory, College of Electromechanical Engineering, Qingdao University, 308 Ningxia Road, Qingdao 266071, PR China

ARTICLE INFO

Article history:
Received 1 April 2012
Received in revised form
28 November 2012
Accepted 24 January 2013
Available online 4 March 2013

Keywords:
Graphene oxide
Calcium alginate
Methylene blue
Adsorption

ABSTRACT

Graphene oxide has been used as an adsorbent in wastewater treatment. However, the dispersibility in aqueous solution and the biotoxicity to human cells of graphene oxide limits its practical application in environmental protection. In this research, a novel environmental friendly adsorbent, calcium alginate immobilized graphene oxide composites was prepared. The effects of pH, contact time, temperature and dosage on the adsorption properties of methylene blue onto calcium alginate immobilized graphene oxide composites were investigated. The equilibrium adsorption data were described by the Langmuir and Freundlich isotherms. The maximum adsorption capacity obtained from Langmuir isotherm equation was 181.81 mg/g. The pseudo-first order, pseudo-second order, and intraparticle diffusion equation were used to evaluate the kinetic data. Thermodynamic analysis of equilibriums indicated that the adsorption reaction of methylene blue onto calcium alginate immobilized graphene oxide composites was exothermic and spontaneous in nature.

1. Introduction

Dyes are widely used in the synthesis, printing, textile, pulp mill, food and cosmetic industries. The estimated annual production of commercially available dyes is approximately 7×10^5 t, including more than 100,000 kinds of dyes (Sharma & Uma, 2010). In China, dyeing wastewater has been released into the environment in large quantities, causing pollution of water and soil. Some dyes and their degradation products are not easily biodegradable and have a toxic, carcinogenic, or mutagenic influence on human beings (Chen, Chen, & Diao, 2010). Therefore, it is necessary to remove dyes prior to their discharge. Several methods such as membrane separation, flocculation, coagulation, ozonatioin, aerobic or anaerobic treatment and adsorption have been explored to remove dyes from dyeing wastewater (Slokar & Le Marechal, 1998). However, among these methods, adsorption is the most widely used technology because it is simple, low cost and effective for removing dyes from waste streams. Various adsorbents, such as rice husk (Li, Du, et al., 2011), garlic peel (Hameed & Ahmad, 2009), pyrolyzed petrified sediment (Aroguz, Gulen, & Evers, 2008), coir pith carbon (Kavitha & Namasivayam, 2007), activated clay (Weng & Pan, 2007), carbon nanotubes (Yao, Xu, Chen, Xu, & Zhu, 2010), activated desert plant (Bestani, Benderdouche, Benstaali, Belhakem, & Addou, 2008), and activated carbon (Karagöz, Tay, Ucar, & Erdem, 2008), have been studied for adsorption of dyes from aqueous solutions.

Graphene and graphene oxide (GO), new types of carbon nanomaterials, have attracted enormous research interests not only in electronics (Eom et al., 2009) and mechanics (Lee, Wei, Kysar, & Hone, 2008), but also in wastewater treatment. It has been used for the adsorption of fluoride ions (Li, Zhang, et al. 2011), heavy metals (As (Mishra & Ramaprabhu, 2011), Cu (Yang et al., 2010), Pb and Cd (Deng, Lü, Li, & Luo, 2010), etc.), dyes (methylene blue (Liu et al., 2012), methyl violet, orange-G, rhodamine-B (Ramesha, Vijayakumar, Muralidhara, & Sampath, 2011), etc.) and express good adsorption property. Nevertheless, in very recent work, Wang et al. (2011) demonstrated that GO has the obvious toxicity to human fibroblast cells when the dose is higher than 50 μg/mL. Based on the hemolysis and WST-8 viability assay results, Liao et al. showed that GO has the toxicity to suspended erythrocytes and human skin fibroblasts (Liao, Lin, Macosko, & Haynes, 2011). So, the difficulty of separating nanosized GO from the effluent may result in the loss of the adsorbent and harmful effects on human being as well as the fauna and flora. These disadvantages may limit its practical application in environmental protection in the future.

Sodium alginate, a water-soluble linear polysaccharide, is a natural occurring carbohydrate polymer composed of α-L-guluronate and β-D-mannuronate residues and has hydrophilic, biocompatiblity, and nontoxic (Liu, Chen, Zhong, & Wu, 2009). The gelling

* Corresponding author. Fax: +86 532 85951842.
E-mail address: liyanhui@tsinghua.org.cn (Y. Li).

0144-8617/$ – see front matter © 2013 Elsevier Ltd. All rights reserved.
http://dx.doi.org/10.1016/j.carbpol.2013.01.094

properties of sodium alginate are mainly achieved by the exchange of sodium ions from the guluronic acid residues with the divalent cations (Ca^{2+}, Sr^{2+}, Ba^{2+}, etc.). The divalent cations bind to the α-L-guluronic acid blocks between two different chains resulting in a three-dimension network (Sarmento et al., 2006). Calcium alginate has been widely used to immobilize activated carbon (Kim, Jin, Park, Kim, & Cho, 2008), carbon nanotubes (Li et al., 2010), titanian nanoparticles (Mahmoodi, Hayati, Arami, & Bahrami, 2011), and maghemite nanoparticles (Rocher, Siaugue, Cabuil, & Bee, 2008) to create adsorbents to remove heavy metals and dyes from aqueous solutions. However, to our knowledge, no study on preparing calcium alginate immobilized graphene oxide (GO/CA) composites used for the removal of dyes has been reported.

In this work, GO/CA fibers were prepared using a sol-gel method and characterized by scanning electron microscope (SEM), transmission electron microscope (TEM) and Fourier Transform infrared spectroscopy (FTIR). The adsorption equilibrium and kinetic studies have been investigated to observe the effects of various process parameters such as pH, contact time, and temperature on methylene blue (MB) removal.

2. Experimental

2.1. Materials

Graphene oxide was prepared from expandable graphite (Henglide Graphite Co., Ltd., Qingdao, China) by a modified Hummers method (Hummers & Offeman, 1958). Expandable graphite (2.5 g) was mixed with a mixture of H_2SO_4 (115 mL, 98 wt %), $KMnO_4$ (15 g) and $NaNO_3$ (2.5 g) in ice bath. The obtained mixture was then kept at 0 °C for 24 h. Then the mixture was stirred at 35 °C for 30 min and slowly diluted with deionized water. The reaction temperature was rapidly increased to 98 °C and kept for 15 min, and the color turned into yellow as 30% H_2O_2 was added to the mixture. Then, the mixture was centrifuged and washed with HCl (5%) and deionized water several times. After drying under room condition, graphene oxide (GO) was obtained.

5 g sodium alginate (AR, Aibi Chemistry Preparation Co., Ltd., Shanghai, China) was dissolved into 350 mL deionized water and stirred for 5 h. 0.26 g GO was added into 50 mL deionized water and ultransonicated for 30 min. Then the GO solution was slowly dropped into the viscous solution of sodium alginate and stirred continuously to form a homogeneous mixed solution. Then, the mixed solution was rapidly injected into 1000 mL 10% $CaCl_2{\cdot}2H_2O$ (AR, Basf Chemical Co., Ltd., Tianjin, China) to form GO/CA fibers. The obtained GO/CA fibers were washed several times with deionized water and then dried in a vacuum freeze drying machine (FD-1-50, Boyikang Laboratory Apparatus Co., Ltd, Beijing, China).

2.2. Characterization of adsorbents

The morphology and surface structure of GO and GO/CA fibers were examined with JSM 6700F scanning electron microscope (SEM) and JEM-2100F transmission electron microscope (TEM). Functional groups of GO and GO/CA were analyzed by a Perkin-Elmer-283FTIR spectrometer over the wave range from 4000 to 400 cm^{-1}.

2.3. Batch adsorption experiments

MB was purchased from Tianjin Red Cliff Chemical Reagent Factory in China and the stock solution (1000 mg/L) was prepared by dissolving the MB in deionized water.

Adsorption experiments were carried out using batch equilibration techniques in a temperature-controlled water bath shaker (SHZ-82A). For adsorption equilibrium experiments, a fixed adsorbent dose (25 mg) was weighed into 100 mL conical flasks containing 50 mL of different initial concentrations (30–80 mg/L) of MB. The mixture was shaken for 5 h at 25 °C until equilibrium was obtained. Then the adsorbent was separated from solution by centrifugation at 7000 rpm for 6 min. The concentration of MB in the solution was measured using a UV–vis spectrophotometer (TU-1810, Beijing Purkinje General Instrument Co., Ltd., China) at 663 nm. The adsorption capacity was calculated using the following equation:

$$q_e = \left(\frac{C_0 - C_e}{m}\right) \times V \quad (1)$$

where C_0 and C_e were initial and equilibrium concentrations of MB (mg/L), respectively, m was the mass of adsorbent (g) and V was volume of the solution (L).

The effect of pH on the adsorption of MB was studied in a pH range of 3.4–10.2 using 50 mL of solutions with MB concentrations of 60 mg/L. The effect of adsorbent dose on the adsorption of MB was conducted by adding different amounts of adsorbents (0.01–0.10 g) into 50 mL of solutions with MB concentration of 80 mg/L. The effect of contact time on the adsorption of MB was carried out in a 2000 mL glass beaker at 25 °C. The aqueous solution (1000 mL) with GO/CA (0.5 g) and MB (40 mg/L) was shaken continuously. The recording time was started when GO/CA was added to the beaker. Aqueous samples (5 mL) were taken from the solution at predetermined time. The filtrate was analyzed and the amount of adsorbed MB at time t, q_t (mg/g), was calculated by:

$$q_t = \left(\frac{C_0 - C_t}{m}\right) \times V \quad (2)$$

where C_t (mg/L) is the MB concentration at time t.

To evaluate the temperature effect on the adsorption, 25 mg adsorbents were added into 50 mL solutions with initial MB concentration ranging from 30 to 80 mg/L. The samples were shaken at 25, 40 and 55 °C, respectively, until the equilibrium was obtained.

GO/CA utilized for the adsorption of initial dye concentration of 80 mg/L was separated from the MB solution. The MB adsorbed GO/CA was washed with deionized water for the removal of any unabsorbed dye. And then, it was put into 50 mL deionized water with pH 1.5. Finally they were shaken for 420 min. The amount of dye desorbed was determined as mentioned before.

3. Results and discussion

3.1. Characterization of materials

Fig. 1a shows the TEM image of GO, it can be seen that GO is transparent film due to its single-atom layered structure. The surface of GO film is wrinkled due to the crumpling and scrolling of graphene sheets. Fig. 1b shows that the dried GO/CA fibers have belt-like structrue. Most GO sheets are embedded into CA. GO/CA composites have a very rough surface and lots of raised strips.

The functional groups of GO and GO/CA were characterized by FT-IR spectra and shown in Fig. 2. The strong peak at 3426 cm^{-1} is assigned to stretching vibration of OH groups. The bands at 1625 and 1400 cm^{-1} indicate the existence of asymmetric and symmetric stretching vibration of C═O groups. The band at 1110 cm^{-1} can be attributed to the appearance of C—O groups. The bands at 621 cm^{-1} reflect the C—H bending vibrations. The peak around at 475 cm^{-1} may correspond to C—O stretching vibration.

3.2. Adsorption isotherms of GO and GO/CA

The adsorption isotherm is usually used to study how the adsorption molecules distribute between the liquid phase and the

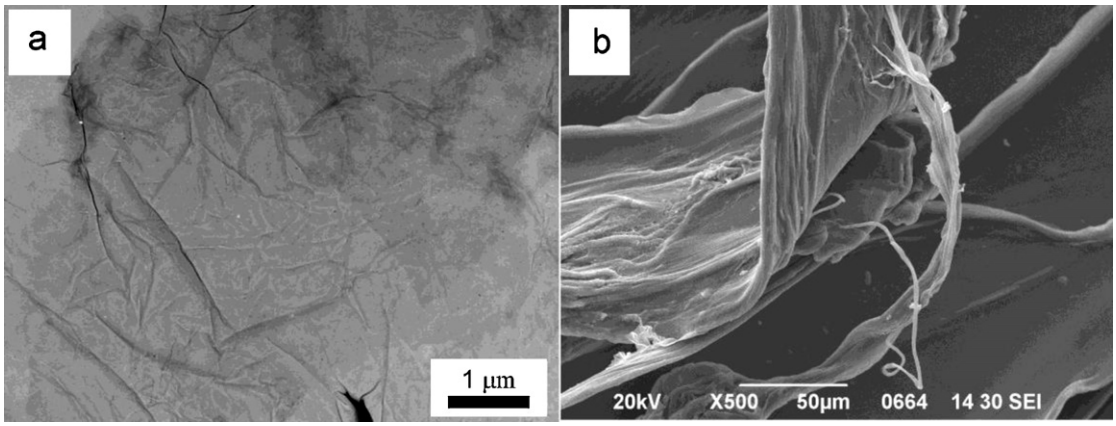

Fig. 1. (a) TEM image of GO, (b) SEM image of GO/CA fibers.

solid phase when the adsorption process reaches an equilibrium state. The adsorption isotherms of GO and GO/CA were presented in Fig. 3. It is clear that MB molecules are more favorably adsorbed onto GO/CA and its sorption capacity attained 140.80 mg/g at an initial concentration of 80 mg/L. The adsorption capacity of GO is 135.44 mg/g at the same conditions. The higher adsorption capacity of GO/CA may be due to that the addition of GO increases the surface area, allowing more functional groups to be exposed, which enhances the adsorption ability of the composites (He, Zhang, & Wang, 2011).

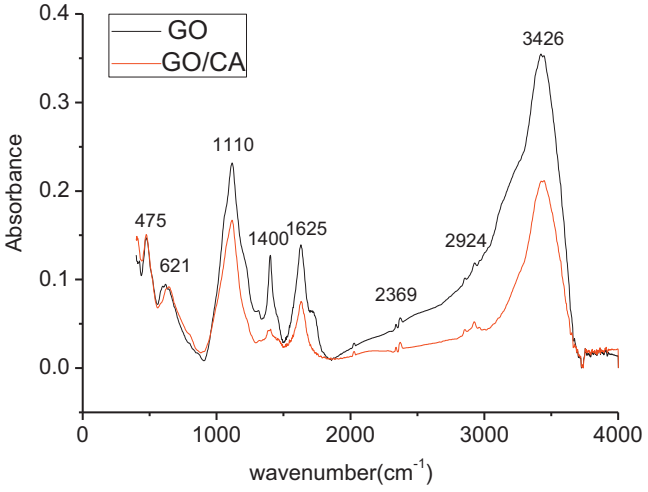

Fig. 2. FTIR spectrum of GO/CA and GO.

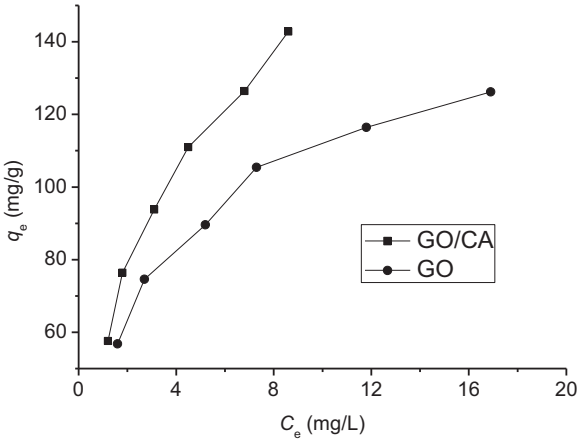

Fig. 3. Adsorption isotherms of MB adsorbed by GO/CA and GO (dose of adsorbent: 0.05 g, temperature: 25 °C, solution concentrations: 30–80 mg/L).

3.3. Effect of adsorbent dose

Fig. 4a shows the effect of the adsorbent dose on the equilibrium adsorption capacity and removal percentage of MB adsorbed by GO/CA. It is apparent that the initial rise in removal percentage with increasing adsorbent dose may be due to availability of more binding sites for adsorption. However, on further increase in the adsorbent dose, the removal percentage changes little because of the unavailability of adsorbate sites due to saturation (Gupta et al., 2010). It can be observed that the MB adsorption capacity decreases with increasing adsorbent. This is because the quantity of dye adsorbed per unit weight of the adsorbent is reduced causing a decrease in the utility of active sites (Aravindhan, Fathima, Rao, & Nair, 2007; Popuri, Vijaya, Boddu, & Abburi, 2009).

3.4. Effect of pH

The initial pH of the solution is an important variable in the whole adsorption process because it can affect the dye adsorption process through changing the surface charge of an adsorbent and the ionization behavior of adsorbent and dye. Fig. 4b shows the effect of the initial pH on the adsorption of MB onto GO/CA. At pH = 3.4, GO/CA has a lower removal percentage (83.75%), which may be due to the protons competition with the dye molecules for the available adsorption sites (Vadivelan & Kumar, 2005). As the pH increases, the removal percentage gradually increases to 88.6–92.7% and is only slightly affected by pH. It may be due to the more functional groups and more binding sites formed on the surface of GO/CA to increase its surface complexation capability (Li et al., 2010).

3.5. Effect of agitation time

The effect of the agitation time on the adsorption process was studied at 40 mg/L initial MB concentration at 25 °C and shown in Fig. 4c. It is obviously that the adsorption rate of MB is rapid at first 60 min, indicating a high affinity between the MB molecules and the GO/CA surface and adsorption occurring mainly on the surface at the beginning. Following this phase, the adsorption rate gradually slows down until the adsorption reaches equilibrium (about 420 min), which may be attributed to the long-range diffusion of dye molecules into the inner cavities of GO/CA (Hu, Qiao, Haghseresht, Wilson, & Lu, 2006).

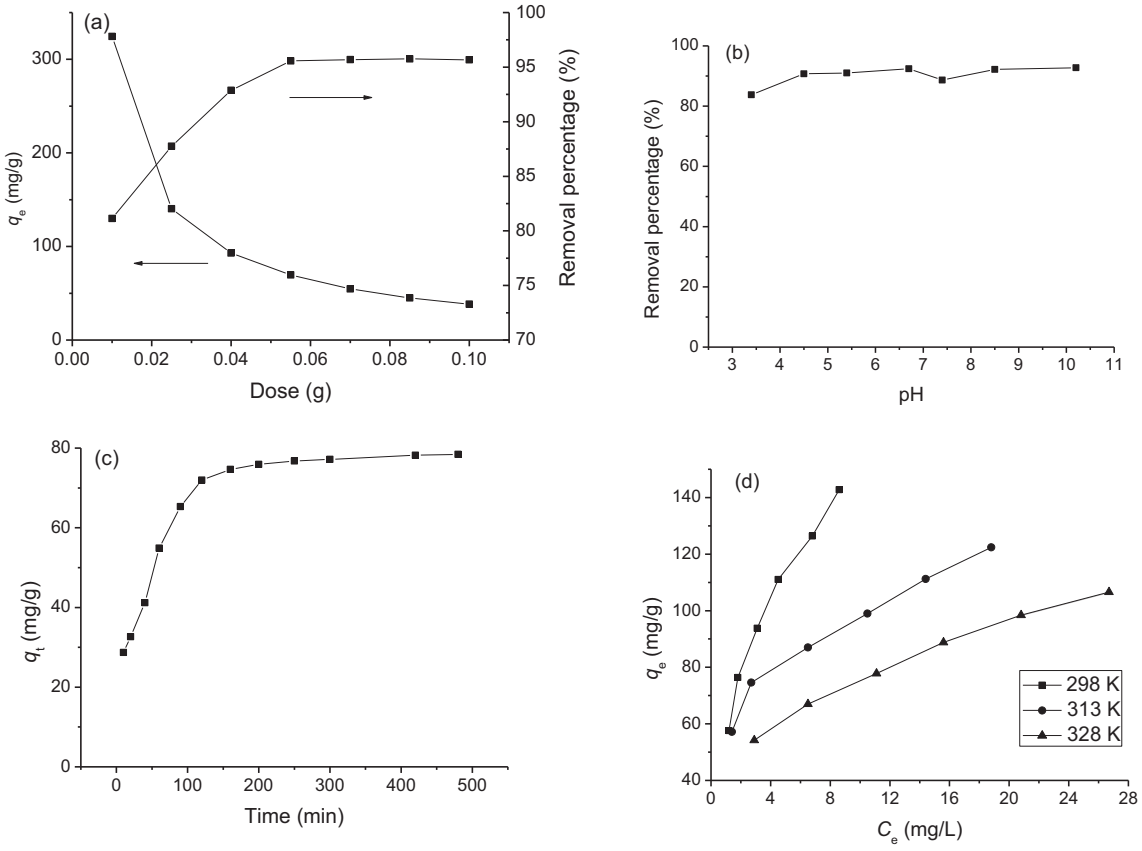

Fig. 4. Effect of different factors on MB adsorbed by GO/CA: (a) dose effect, (b) pH effect, (c) agitation time effect, (d) temperature effect.

3.6. Effect of temperature

To determine the effect of temperature, adsorption experiments were carried out at 25, 40 and 55 °C, respectively. The results were shown in Fig. 4d. The adsorption capacity increases with decrease in temperature. The maximum adsorption capacity decreases from 163.93 to 140.85 mg/g with the increase in temperature from 25 to 55 °C, which illustrates that the adsorption process of MB onto GO/CA is exothermic.

3.7. Equilibrium modeling

Several mathematical models have been used for describing equilibrium studies for the removal of pollutants by adsorption. The selection of an isotherm model depends on the nature and type of the system (Sharma, Uma Sinha, & Upadhyay, 2010). The Langmuir model and The Freundlich model are the most commonly used models to study the adsorption equilibrium.

The Langmuir model supposes that uptake of dyes occurs on a homogenous surface by monolayer adsorption. The equation of the Langmuir isotherm is as follows (Langmuir, 1918):

$$\frac{C_e}{q_e} = \frac{C_e}{q_{\max}} + \frac{1}{q_{\max}\ k_L} \tag{3}$$

where $q_{\max}$ (mg/g) is the maximum adsorption capacity corresponding to complete monolayer coverage, k_L (L/g) is a constant related to adsorption capacity and energy of adsorption. A straight line was obtained when C_e/q_e was plotted against C_e. The values of $q_{\max}$ and k_L were calculated from the slopes and intercepts. They are 144.92 mg/g and 0.37 L/g for GO and 181.81 mg/g and 0.67 L/g for GO/CA. The higher correlation coefficients of R^2 (0.9976 for GO and 0.9921 for GO/CA) suggest that the Langmuir model can be applied to fitting the experimental data. The maximum adsorption capacities of GO and GO/CA were compared with other commonly used adsorbents (Table 1). The adsorption capacity of GO is only a little bit lower than that of graphene. However, it was higher than other adsorbents. After composited with CA, GO/CA not only has the improved adsorption capacity, but also can be easily removed from aqueous solution by applying conventional separation method. The results reveal the promising application of GO/CA to be an effective adsorbent for removing dyes.

The Freundlich equation is an empirical equation based on adsorption on a heterogeneous surface. The equation is commonly represented by (Freundlich, 1906):

$$Lnq_e = Lnk_F + \frac{1}{n}Lnc_e \tag{4}$$

where k_F (L/g) and n are the Freundlich constants, indicating the adsorption capacity and the adsorption intensity, respectively. A straight line was obtained when Lnq_e was plotted against LnC_e and n and k_F were obtained from the slopes and intercepts. The calculated values of n and k_F are 2.99 and 51.32 L/g for GO and 2.28 and 56.11 L/g for GO/CA. Although the correlation coefficients R^2 (0.98376 for GO and 0.9777 for GO/CA) of the Freundlich equation are lower than those of the Langmuir equation, the Freundlich equation can also be used to roughly evaluate the experimental data. The values of n in the range of 1–10 suggest favorable adsorption for MB onto GO and GO/CA. The high values of k_F indicate that both GO and GO/CA have high adsorption capacity and affinity for MB molecules (Dogan, Mustafa, Eda, Sema, & Aysüegu1, 2007).

3.8. Kinetic studies

To evaluate the kinetic mechanism of the adsorption process, the pseudo-first-order (Dogan, Alkan, Demirbas, Ozdemir, & Ozmetin,

Table 1
Adsorption capacities (q_m calculated from Langmuir model) of MB adsorbed by various adsorbents.

Adsorbent	Experimental conditions					Ref.
	Dose (g/L)	pH	Temp. (°C)	Concn. (mg/L)	q_{max} (mg/g)	
Rice husk	10.0	N/A	30	60–100	9.83	Sharma and Uma (2010)
Garlic peel	3.0	N/A	30	25–200	82.64	Hameed and Ahmad (2009)
Pyrolyzed petrified sediment	10.0	7.0	30	10–60	2.39	Aroguz et al. (2008)
Coir pith carbon	6.0	N/A	35	10–40	5.87	Kavitha and Namasivayam (2007)
Activated clay	0.2	5.5	25	N/A	91.23	Weng and Pan (2007)
Carbon nanotubes	0.3	7.0	25	5–40	46.20	Yao et al. (2010)
Activated desert plant	4.0	6.94	24	100–1000	23.00	Bestani et al. (2008)
Graphene	0.5	N/A	20	20–120	153.85	Liu et al. (2012)
GO	0.5	5.4	25	20–70	144.92	This study
GO/CA	0.5	5.4	25	20–70	181.81	This study

2006), pseudo-second-order (Ho & Chiang, 2001) and intraparticle diffusion models (Uzun, 2006) were applied to fit the experimental data in this work.

The pseudo-first-order rate model is as follows:

$$\log(q_e - q_t) = \log_e - \frac{k_1}{2.303}t \quad (5)$$

where k_1 (1 min^{-1}) is the Lagergren rate constant of adsorption, q_e (mg/g) is the maximum adsorption capacity, and q_t (mg/g) is the amount of adsorption at time t (min). The values of k_1 and q_e were determined from the intercept and the slope of the plot of log ($q_e - q_t$) versus t (Fig. 5a) and shown in Table 2. The R^2 value is low and the calculated q_e value is much lower than the experimental value, indicating that the pseudo-first-order rate model does not fit this adsorption process.

The pseudo-second-order rate model is expressed:

$$\frac{t}{q_t} = \frac{1}{2k_2 q_e^2} + \frac{1}{q_e} \quad (6)$$

where k_2 is the pseudo second-order rate constant of adsorption (g/mg min). k_2 and q_e (Table 2) were determined from the intercept and the slope of the plot of t/q_t versus t (Fig. 5b). The correlation coefficients of R^2 are high and the calculated values of q_e are in accordance with the experiment values, indicating that the adsorption of MB onto GO/CA fits the pseudo second-order rate model. This means that the overall rate of MB adsorption process seems to be controlled by the chemical process through sharing of electrons or by covalent forces through exchanging of electrons between adsorbent and adsorbate (Nuhoglu & Malkoc, 2009).

The intraparticle diffusion model is represented in the following form:

$$q_t = k_{id} t^{1/2} + C_i \quad (7)$$

where k_{id} is an intraparticle diffusion rate constant, and C_i is related to the thickness of the boundary layer. The intraparticle diffusion parameters (Table 2) could be obtained from the plot of q_t versus $t^{1/2}$. If the regression of q_t versus $t^{1/2}$ is linear and passes through the origin, it indicates that the intraparticle diffusion is the sole rate-limiting step (Zhu et al., 2011). Fig. 5c shows that the plots of q_t versus $t^{1/2}$ have a multilinearity characterization, indicating that two steps occurred in the adsorption process. The first sharp section is the external surface adsorption or instantaneous adsorption stage. The second subdued portion is the gradual adsorption stage, where intra-particle diffusion is rate-controlled. The larger slope of the first sharp section indicates that the rate of MB removal is higher in the beginning stage due to the instantaneous availability of large surface area and active adsorption sites. The lower slope of the second subdued portion is due to that the decreased concentration gradients make dye molecule diffusion in the micropores of adsorbent take long time, thus leading to a low removal rate (Ma, Jia, Jing, Yao, & Sun, 2012).

Table 2
Kinetic parameters for the adsorption of MB absorded by GO/CA.

Kinetic model	Parameters	Values
Pseudo-first-order	q_e (mg/g)	26.98
	k_1 (1 min^{-1}) · 10^{-3}	145.01
	R^2	0.7745
Pseudo-second-order	q_e (mg/g)	78.92
	K_2 (g/mg·min)·10^{-3}	0.52
	R^2	0.9982
Intra-particle diffusion	$k_{id,1}$	4.64
	C_1	13.54
	R_1^2	0.9419
	$k_{id,2}$	0.12
	C_2	71.94
	R_2^2	0.9168

3.9. Thermodynamic studies

Thermodynamic parameters such as standard free energy change, enthalpy change and entropy change were calculated to evaluate the thermodynamic feasibility and the spontaneous nature of the adsorption process. Thermodynamic parameters can be calculated from the variation of the thermodynamic equilibrium constant K_0 with the change in temperature (Li et al., 2005). For adsorption reactions, K_0 is defined as follows:

$$K_0 = \frac{a_s}{a_e} = \frac{v_s}{v_e}\frac{C_s}{C_e} \quad (10)$$

where a_s is the activity of adsorbed MB, a_e is the activity of MB in solution at equilibrium, C_s is the amount of dye adsorbed by per mass of GO/CA (mmol/g), v_s is the activity coefficient of the adsorbed MB and v_e is the activity coefficient of MB in solution. As dye concentration in the solution decreases and approaches zero, K_0 can be obtained by plotting $Ln(C_s/C_e)$ vs. C_s and extrapolating C_s to zero (Table 3)

The average standard enthalpy change (ΔH^0) is obtained from Van't Hoof equation:

$$LnK_0(T_3) - LnK_0(T_1) = \frac{-\Delta H^0}{R}\left(\frac{1}{T_3} - \frac{1}{T_1}\right) \quad (11)$$

where T_3 and T_1 are two different temperatures.

Table 3
Thermodynamic parameters for the adsorption of MB adsorbed by GO/CA.

Thermodynamic constant	Temperature (K)		
	298	313	333
K_0	108.94	218.20	74.11
ΔG_0 (kJ/mol)	−11.66	−14.07	−11.79
ΔH^0 (kJ/mol)	−5.27	−5.27	−5.27
ΔS^0 (J/mol•K)	21.63	28.10	19.87

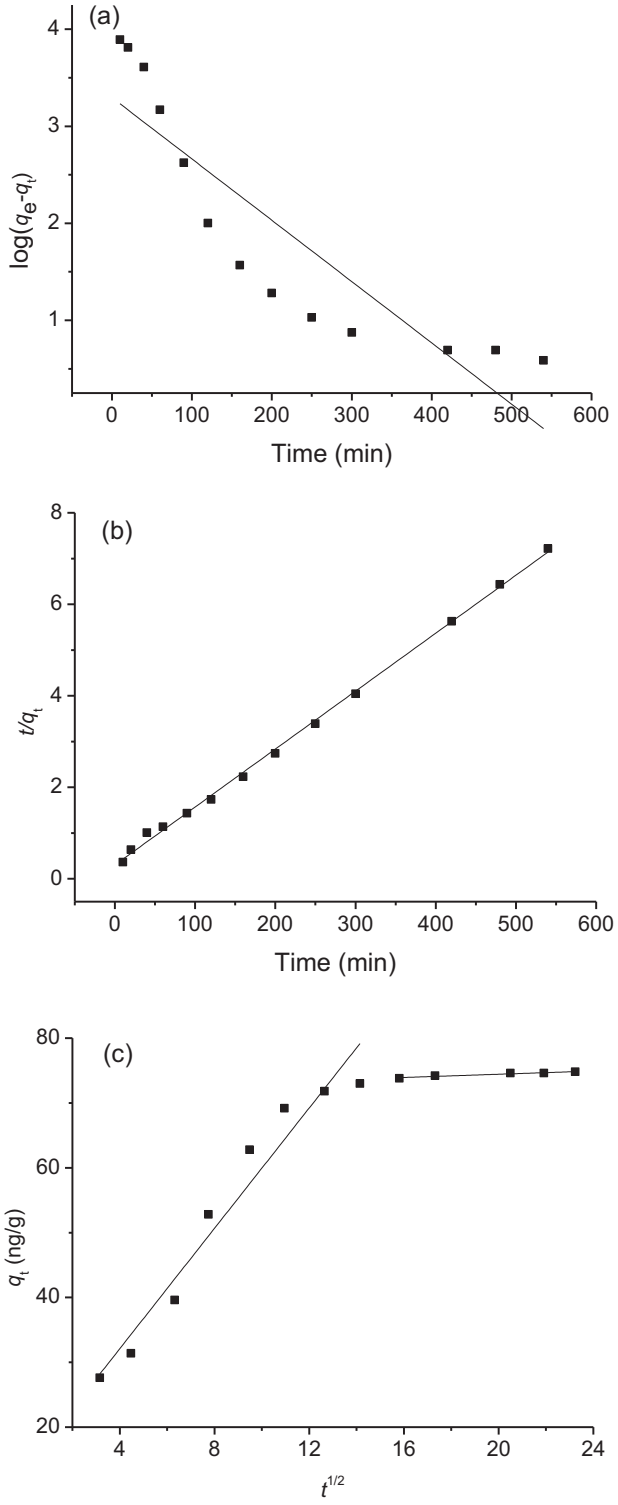

Fig. 5. Adsorption kinetics of MB adsorbed by GO/CA: (a) pseudo-first-order model, (b) pseudo-second-order model, (c) intraparticle diffusion model.

The adsorption standard free energy changes (ΔG^0) can be calculated according to:

$$\Delta G^0 = -RTLnK_0 \quad (12)$$

where R is the universal gas constant (8.345 J/K mol) and T is the temperature in Kelvin. The standard entropy change (ΔS^0) can be obtained by:

$$\Delta S^0 = -\frac{\Delta G^0 - \Delta H^0}{T} \quad (13)$$

The thermodynamic parameters were listed in Table 3. Negative value of ΔH^0 suggests that the interaction of MB adsorbed by GO/CA is exothermic process, which supported by the decreasing adsorption of MB with the increase in temperature. The positive values of ΔS^0 demonstrates the increased randomness at the solid-solute interface and the affinity of GO/CA for the MB (Aroguz et al., 2008). The negative values of ΔG^0 reveal the fact that adsorption process is spontaneous. It was reported that the values of ΔG^0 in between 0 and −20 kJ/mol indicate a physisorption process, while the values in between −80 to −400 kJ/mol correspond to chemisorption process (Fernandes, Almeida, Debacher, & Sierra, 2010; Weng, Lin, & Tzeng, 2009). The values of ΔG^0 in Table 3 are −11.66, −14.07, and −11.79 kJ/mol, respectively, suggesting that adsorption of MB onto GO/CA is a physisorption process.

3.10. Desorption studies

The repeated availability is an important factor for an advanced adsorbent. Desorption studies help to elucidate the nature of adsorption and access the regeneration performance of the spent adsorbent (Abdallah & Taha, 2012). In order to investigate the possibility of desorption of MB from GO/CA, desorption experiment was performed at solution pH of 1.5. The desorption efficiency can reach 78.6% at pH 1.5. The higher desorption efficiency at acidic condition is due to that excessive H^+ ions compete the activated adsorption sites on GO/CA with the cationic MB molecules and replace the adsorbed MB molecules through ion exchange resulting in desorbing dye molecules from GO/CA.

4. Conclusions

A new efficient and eco-friendly adsorbent of GO/CA was prepared in this work. GO/CA has high adsorption capacity and removal efficiency in the whole studied pH range and it can be separated from aqueous solution easily, which avoids the secondary pollution caused by micro-sized GO. The adsorption process followed both the Langmuir and the Freundlich isotherm equations but the former was more suitable, suggesting that uptake of MB occurred on the homogenous surface of GO/CA by monolayer adsorption. The kinetic adsorption followed a pseudo-second-order kinetic model and intraparticle diffusion was indicated to play a major role in MB adsorption. The increased adsorption capacity with increasing temperature and the calculated thermodynamic parameters showed that the adsorption process was thermodynamically favorable, spontaneous and exothermic in nature.

Acknowledgements

This work was supported by the National Natural Science Foundation of China (20975056), SRF for ROCS, SEM, Natural Science Foundation of Qingdao (12-1-4-2-23-jch), Program for Changjiang Scholars and Innovative Research Team in University (IRT0970) and National Key Basic Research Development Program of China (973 special preliminary study plan, grant no.: 2012CB722705).

References

Abdallah, R., & Taha, S. (2012). Biosorption of methylene blue from aqueous solution by nonviable *Aspergillus fumigates*. *Chemical Engineering Journal*, *195/196*, 69–76.

Aravindhan, R., Fathima, N. N., Rao, J. R., & Nair, B. U. (2007). Equilibrium and thermodynamic studies on the removal of basic black dye using calcium alginate beads. *Colloids and Surfaces A*, *299*, 232–238.

Aroguz, A. Z., Gulen, J., & Evers, R. H. (2008). Adsorption of methylene blue from aqueous solution on pyrolyzed petrified sediment. *Bioresource Technology*, *99*, 1503–1508.

Bestani, B., Benderdouche, N., Benstaali, B., Belhakem, M., & Addou, A. (2008). Methylene blue and iodine adsorption onto an activated desert plant. *Bioresource Technology*, *99*, 8441–8444.

Chen, M., Chen, Y., & Diao, G. W. (2010). Adsorption kinetics and thermodynamics of methylene blue onto p-tert-butyl-calix[4,6,8]arene-bonded silica gel. *Journal of Chemical and Engineering Data*, *55*, 5109–5116.

Deng, X. J., Lü, L. L., Li, H. W., & Luo, F. (2010). The adsorption properties of Pb(II) and Cd(II) on functionalized graphene prepared by electrolysis method. *Journal of Hazardous Materials*, *183*, 923–930.

Dogan, K., Mustafa, T., Eda, A., Sema, T., & Aysüegu1, F. (2007). Adsorption equilibrium and kinetics of reactive black 5 and reactive red 239 in aqueous solution onto surfactant-modified zeolite. *Journal of Chemical and Engineering Data*, *52*, 1615–1620.

Dogan, M., Alkan, M., Demirbas, O., Ozdemir, Y., & Ozmetin, C. (2006). Adsorption kinetics of maxilon blue GRL onto sepiolite from aqueous solutions. *Chemical Engineering Journal*, *124*, 89–101.

Eom, D., Prezzi, D., Rim, K. T., Zhou, H., Lefenfeld, M., Xiao, S., et al. (2009). Structure and electronic properties of graphene Nanoislands on Co(0 0 0 1). *Nano Letters*, *9*, 2844–2848.

Fernandes, A. N., Almeida, C. A. P., Debacher, N., & Sierra, M. M. S. (2010). Isotherm and thermodynamic data of adsorption of methylene blue from aqueous solution onto peat. *Journal of Molecular Structure*, *982*, 62–65.

Freundlich, H. M. F. (1906). Über die adsorption in lösungen. *Zeitschrift für Physikalische Chemie*, *57A*, 385–470.

Gupta, V. K., Jain, R., Siddiqui, M. N., Saleh, T. A., Agarwal, S., Malati, S., et al. (2010). Equilibrium and thermodynamic studies on the adsorption of the dye rhodamine-B onto mustard cake and activated carbon. *Journal of Chemical and Engineering Data*, *55*, 5225–5229.

Hameed, B. H., & Ahmad, A. A. (2009). Batch adsorption of methylene blue from aqueous solution by garlic peel, an agricultural waste biomass. *Journal of Hazardous Materials*, *164*, 870–875.

He, Y. Q., Zhang, N. N., & Wang, X. D. (2011). Adsorption of graphene oxide/chitosan porous materials for metal ions. *Chinese Chemical Letters*, *2*, 859–862.

Ho, Y. S., & Chiang, C. C. (2001). Sorption studies of acid dye by mixed sorbents. *Adsorption: Journal of the International Adsorption Society*, *7*, 139–147.

Hu, Q. H., Qiao, S. Z., Haghseresht, F., Wilson, M. A., & Lu, G. Q. (2006). Adsorption study for removal of basic red dye using bentonite. *Industrial and Engineering Chemistry Research*, *45*, 733–738.

Hummers, W. S., Jr., & Offeman, R. E. (1958). Preparation of graphitic oxide. *Journal of the American Chemical Society*, *80*, 1339.

Karagöz, S., Tay, T., Ucar, S., & Erdem, M. (2008). Activated carbons from waste biomass by sulfuric acid activation and their use on methylene blue adsorption. *Bioresource Technology*, *99*, 6214–6222.

Kavitha, D., & Namasivayam, C. (2007). Experimental and kinetic studies on methylene blue adsorption by coir pith carbon. *Bioresource Technology*, *98*, 14–21.

Kim, T. Y., Jin, H. J., Park, S. S., Kim, S. J., & Cho, S. Y. (2008). Adsorption equilibrium of copper ion and phenol by powdered activated carbon, alginate bead and alginate-activated carbon bead. *Journal of Industrial and Engineering Chemistry*, *14*, 714–719.

Langmuir, I. (1918). The adsorption of gases on plane surfaces of glass, mica and platinum. *Journal of the American Chemical Society*, *40*, 1361–1403.

Lee, C., Wei, X., Kysar, J. W., & Hone, J. (2008). Measurement of the elastic properties and intrinsic strength of monolayer graphene. *Science*, *321*, 385–388.

Li, Y. H., Di, Z., Ding, J., Wu, D., Luan, Z., & Zhu, Y. (2005). Adsorption thermodynamic, kinetic and desorption studies of Pb^{2+} on carbon nanotubes. *Water Research*, *39*, 605–609.

Li, Y. H., Du, Q., Liu, T., Qi, Y., Zhang, P., Wang, Z., et al. (2011). Preparation of activated carbon from *Enteromorpha* prolifera and its use on cationic red X-GRL removal. *Applied Surface Science*, *257*, 10621–10627.

Li, Y. H., Liu, F. Q., Xia, B., Du, Q. J., Zhang, P., Wang, D. C., et al. (2010). Removal of copper from aqueous solution by carbon nanotube/calcium alginate composites. *Journal of Hazardous Materials*, *177*, 876–880.

Li, Y. H., Zhang, P., Du, Q., Peng, X., Liu, T., Wang, Z., et al. (2011). Adsorption of fluoride from aqueous solution by graphene. *Journal of Colloid and Interface Science*, *363*, 348–354.

Liao, K. H., Lin, Y. S., Macosko, C. W., & Haynes, C. L. (2011). Cytotoxicity of graphene oxide and graphene in human erythrocytes and skin fibroblasts. *ACS Applied Materials and Interfaces*, *3*, 2607–2615.

Liu, T., Li, Y. H., Du, Q., Sun, J., Jiao, Y., Yang, G., et al. (2012). Adsorption of methylene blue from aqueous solution by graphene. *Colloids and Surfaces B*, *90*, 197–203.

Liu, Y. S., Chen, S. M., Zhong, L., & Wu, G. Z. (2009). Preparation of high-stable silver nanoparticle dispersion by using sodium alginate as a stabilizer under gamma radiation. *Radiation Physics and Chemistry*, *78*, 251–255.

Ma, J., Jia, Y., Jing, Y., Yao, Y., & Sun, J. (2012). Kinetics and thermodynamics of methylene blue adsorption by cobalt-hectorite composite. *Dyes and Pigments*, *93*, 1441–1446.

Mahmoodi, N. M., Hayati, B., Arami, M., & Bahrami, H. (2011). Preparation, characterization and dye adsorption properties of biocompatible composite (alginate/titania nanoparticle). *Desalination*, *275*, 93–101.

Mishra, A. K., & Ramaprabhu, S. (2011). Functionalized graphene sheets for arsenic removal and desalination of sea water. *Desalination*, *282*, 39–45.

Nuhoglu, Y., & Malkoc, E. (2009). Thermodynamic and kinetic studies for environmentaly friendly Ni(II) biosorption using waste pomace of olive oil factory. *Bioresource Technology*, *100*, 2375–2380.

Popuri, S. R., Vijaya, Y., Boddu, V. M., & Abburi, K. (2009). Adsorptive removal of copper and nickel ions from water using chitosan coated PVC beads. *Bioresourse Technology*, *100*, 194–199.

Ramesha, G. K., Vijayakumar, A., Muralidhara, H. B., & Sampath, S. (2011). Graphene and graphene oxide as effective adsorbents towards anionic and cationic dyes. *Journal of Colloid and Interface Science*, *361*, 270–277.

Rocher, V., Siaugue, J. M., Cabuil, V., & Bee, A. (2008). Removal of organic dyes by magnetic alginate beads. *Water Research*, *42*, 1290–1298.

Sarmento, B., Martins, S., Ribeiro, A., Veiga, F., Neufeld, R., & Ferreira, D. (2006). Development and comparison of different nanoparticulate polyelectrolyte complexes as insulin carriers. *International Journal of Peptide Research and Therapeutics*, *12*, 131–138.

Sharma, Y. C., & Uma. (2010). Optimization of parameters for adsorption of methylene blue on a low-cost activated carbon. *Journal of Chemical and Engineering Data*, *55*, 435–439.

Sharma, Y. C., Uma Sinha, A. S. K., & Upadhyay, S. N. (2010). Characterization and adsorption studies of *Cocos nucifera* L. activated carbon for the removal of methylene blue from aqueous solutions. *Journal of Chemical and Engineering Data*, *55*, 2662–2667.

Slokar, Y. M., & Le Marechal, A. M. (1998). Methods of decoloration of textile wastewaters. *Dyes and Pigments*, *37*, 335–356.

Uzun, I. (2006). Kinetics of the adsorption of reactive dyes by chitosan. *Dyes and Pigments*, *70*, 76–83.

Vadivelan, V., & Kumar, K. V. (2005). Equilibrium, kinetics, mechanism, and process design for the sorption of methylene blue onto rice husk. *Journal of Colloid Interface Science*, *286*, 90–100.

Wang, K., Ruan, J., Song, H., Zhang, J., Wo, Y., & Cui, D. (2011). Biocompatibility of graphene oxide. *Nanoscale Research Letters*, *6*, 1–8.

Weng, C. H., & Pan, Y. F. (2007). Adsorption of a cationic dye (methylene blue) onto spent activated clay. *Journal of Hazardous Materials*, *144*, 355–362.

Weng, C. H., Lin, Y. T., & Tzeng, T. W. (2009). Removal of methylene blue from aqueous solution by adsorption onto pineapple leaf powder. *Journal of Hazardous Materials*, *170*, 417–424.

Yang, S. T., Chang, Y. L., Wang, H. F., Liu, G. B., Chen, S., Wang, Y. W., et al. (2010). Folding/aggregation of graphene oxide and its application in Cu^{2+} removal. *Journal of Colloid Interface Science*, *351*, 122–127.

Yao, Y., Xu, F., Chen, M., Xu, Z., & Zhu, Z. (2010). Adsorption behavior of methylene blue on carbon nanotubes. *Bioresourse Technology*, *101*, 3040–3046.

Zhu, H. Y., Fu, Y. Q., Jiang, R., Jiang, J. H., Xiao, L., & Zeng, G. M. (2011). Adsorption removal of congo red onto magnetic cellulose/Fe_3O_4/activated carbon composite: Equilibrium, kinetic and thermodynamic studies. *Chemical Engineering Journal*, *173*, 494–502.